

DESCRIPTIONCALIBRATION-FREE OPTICAL CHEMICAL SENSORS

5 The subject invention was made with government support under a research project supported by the Department of Energy Ocean Margins Program Grant No. DOE-DEFG03-94ER6224. The government has certain rights in this invention.

Background of the Invention

10 Research on optical chemical sensors blossomed over the past 15-20 years as a result of the availability of novel and inexpensive waveguides and the ever-increasing need for sensors for a wide range of chemical applications. Most chemical sensors however require calibration since sensor response is not consistent between sensors nor is it stable over time.

15 Reagent-based Optical Chemical Sensors (hereafter referred to as ROCS) generated substantial excitement early on in their development because they promised improved performance and versatility over their electrochemical sensor analogs. These potential advantages included greater stability and selectivity and a simple, characterizable response. But, after nearly 20 years of research and development, these advantages have yet to be fully realized ^{1,2}.

20 The majority of ROCS use fiber optics to direct light into a small membrane-enclosed volume, resulting in single-ended electrode-like probes³. In most ROCS designs, a colorimetric or fluorimetric reagent is entrapped within the membrane at the fiber tips. The membrane serves a variety of important purposes- it contains and protects the analyte-selective reagent, it provides an additional level of selectivity for groups of different
25 compounds (e.g. gases, hydrophilic or hydrophobic species), and it acts as a diffuse reflector of the light transmitted through, or emitted from, the selective reagent. Chemical sensing is generally accomplished by simply monitoring the change in light intensity in the presence of the analyte of interest. Light intensity changes unrelated to the analyte such as light source fluctuations or changes in the fiber optic transmission are compensated for by using a

reference light intensity at a wavelength insensitive to the analyte concentration. Even so, these ROCS designs have significant stability problems that primarily originate from the changes in the composition of the entrapped reagent chemistry¹. To improve ROCS performance, researchers began investigating methods for renewing the reagent^{4,5}.

Although steps have been taken in achieve consistency and stability among optical chemical sensors, a calibration-free sensor displaying long-term stability and an identical response from sensor to sensor has not yet been described. A need therefore exists for such a calibration-free sensor that can be applied to a wide range of biomedical, industrial and environmental applications.

All patents, patent applications, provisional patent applications and publications referred to or cited herein, or from which a claim for benefit of priority has been made, are incorporated by reference in their entirety to the extent they are not inconsistent with the explicit teachings of the specification.

Brief Summary of the Invention

The subject invention involves an apparatus for taking absorbance-based chemical measurements which requires no calibration. The subject apparatus comprises a reagent-based optical chemical sensor/analyzer having an analyte-selective reagent which transduces analyte concentration into an optical signal, the apparatus also comprises a means for renewing the reagent, a means for allowing the reagent to reach equilibrium with the analyte and, means for calculating response from a ratio of reagent solution absorbance which is determined relative to a blank solution. This calibration-free system displays a response which is consistent among sensors/analyzers and shows no drift over time. Methods of taking absorbance-based chemical measurements using the calibration-free apparatus of the subject invention are also described.

Brief Description of the Drawings

Figure 1 shows a single-ended renewable-reagent $p\text{CO}_2$ sensor design. Note: individual components are not drawn to scale.

Figure 2 shows a cut away view of a Submersible Autonomous Moored Instrument for CO_2 (SAMI- CO_2) sensor design based on a membrane-equilibrator and fiber optic flow cell.

Figure 3 shows the absorbance spectra of the acid (HL-) and base (L2-) forms of the sulfonephthalien indicator bromothymol blue used in a preferred embodiment of the calibration-free apparatus of the subject invention. The total indicator concentration was $\sim 9.0 \times 10^{-5} \text{ M}$.

Figure 4 shows the response of three different SAMI- CO_2 obtained over ~ 1 week period in October 1997 (O-SAMI 5, \square -SAMI 6, Δ -SAMI 7). The solid curve represents the best fit to the average of the three SAMI responses at each $p\text{CO}_2$. Curves were fit to the equation $R_{\text{CO}_2} = a(\log p\text{CO}_2)^2 + b(\log p\text{CO}_2) + c$. Coefficients from the individual curve fits are given in Table 1 and comparisons of $p\text{CO}_2$ s are calculated from the different SAMI curves are shown in Table 2.

Figure 5 shows SAMI absorbances (top) and absorbances ratio A_R (bottom) used to calculated R_{CO_2} in Figure (O-SAMI 5, \square -SAMI 6, Δ -SAMI 7).

Figure 6 shows the experimental and theoretical temperature response at 325 (\square) and 506 μatm (O). The theoretical curves (solid lines) at 325 and 506 μatm have slopes of 0.0071 and 0.0076 R_{CO_2} units $^\circ\text{C}^{-1}$, respectively. The experimental data curves (not shown) at 325 μatm and 506 μatm have slopes of 0.0058 and 0.0065 R_{CO_2} units $^\circ\text{C}^{-1}$, respectively.

Figure 7 shows the SAMI 5 response curves for data from 10/29/97 (Figure 4) (O) and 74 days later on 1/11/98 (\square). The 10/29/97 and 1/11/98 regression curves are shown as solid and dashed lines, respectively. Coefficients from the curves fits are given in Table 1.

5 Figure 8 shows the difference in $p\text{CO}_2$ determined at a single location but at two different depths on an ocean mooring off Cape Hatteras, North Carolina. The data were first low pass filtered to improve the figure clarity (reduced short-term variability). The $\Delta p\text{CO}$ is equal to SAMI 5 (10 m)-SAMI 6 (22m). The difference is calculated over the period when both instruments were operational (SAMI 5 stopped functioning near year day 50 due to an
10 electronic problem).

Detailed Description of the Invention

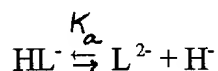
The subject invention involves a device for taking absorbance-based chemical measurements. The subject device is calibration-free displaying a consistent response between
15 sensors/analyzers and showing no drift over time.

Reagent-based optical chemical sensors (ROCS) utilize an analyte-selective reagent to transduce analyte concentration into an optical signal. Light is used to generate and quantify the optical signal. Thus, changes in analyte concentration within the system are detected by monitoring the change in light intensity of the analyte-selective reagent in the
20 presence of the analyte. To achieve a calibration-free reagent-based optical chemical sensor a typical sensor must be run under the following conditions: a) the analyte-selective reagent, or sensing solution, is renewable, b) the analyte-selective reagent is allowed to reach equilibrium with the analyte and, c) the sensor response is calculated from a ratio of the reagent absorbances which are determined relative to a blank solution.

25 Sensors/analyzers suitable for use in the subject invention include any device whose analytical reaction is based upon the creation of two light absorbing forms of a selective reagent which absorb light at different wavelengths. As used herein, sensors are reagent-based optical chemical devices used *in situ*, analyzers do not operate *in situ* but receive samples to be analyzed independently.

In an exemplified embodiment of the calibration-free device of the subject invention a Submersible Autonomous Moored Instrument for CO₂ (SAMI-CO₂) is used as the sensor. The SAMI-CO₂ design was based upon previous CO₂ sensor designs which used a colorimetric pH indicator entrapped within a gas permeable membrane⁶. However, unlike previous sensors, the reagent is renewed during each measurement cycle. The original single-ended probe design is shown in Figure 1^{7,8}. Briefly, the sensor comprises a reagent delivery capillary tube 10, a reagent exit capillary tube 12, fiber optic from source 14, fiber optic to detection system 16, white silicone rubber membrane 18, white silicone sealant 20, epoxy sealant 22, an o-ring 24, a sensor stainless steel housing 26, and a fiber optic and capillary tubing cable 28. The sensor outer diameter ~1 mm. The sensor was subsequently redesigned, finally evolving into a transmission geometry (Figure 2). The SAMI-CO₂ sensor is comprised of a membrane equilibrator attached to a fiber optic flow cell (Figure 2) (the sensor dimensions and other specifications have been reported previously)⁹. Briefly, the sensor in Figure 2 comprises a reagent inlet 30, an equilibrator support 32, a silicone membrane equilibrator 34, a fiber optic cable 36 and a reagent outlet 38.

In operation, ambient CO₂, or analyte, diffuses through a tubular silicone rubber membrane into a sulfonephthalein (bromothymol blue (BTB)) indicator solution or analyte-selective reagent. The diffusion of CO₂ into the indicator solution leads to the formation of carbonic acid which changes the solution pH thereby establishing the equilibrium concentrations of the acid (HL⁻) and the base (L²⁻) forms of the indicator:



The acid form of the solution absorbs light at 434 nm. The base form of the solution absorbs light at 620 nm. The fully protonated form of the diprotic sulfonephthalein indicator (H₂L, pK_a=2) is not present in significant amounts at the indicator solution pH (around pH 7).

To achieve the subject calibration-free system, the analyte-selective reagent of the optical chemical sensor/analyzer must be renewable. A variety of pumps and valves are available for supplying new reagent to a sensor/analyzer. A solenoid pump and valve are used

in a preferred embodiment. Additionally, peristaltic pumps, syringe pumps, positive displacement pumps, and valves, such as, pinch valves can be used for this purpose.

In the calibration-free system of the subject invention, the analyte-selective reagent must be allowed to reach equilibrium with the analyte (e.g. see previous reaction). This is accomplished by allowing the reagent and analyte suitable time to reach equilibrium. Therefore, a pumping system designed to move reagent through the system must be calibrated to allow adequate time for the indicator solution and analyte to equilibrate.

For example, in an exemplified embodiment in which a SAMI-CO₂ is the sensor, indicator solution stored in an isolated reagent bag was pumped into the membrane for each measurement. In initial studies using the sensor design in Figure 1, the indicator solution was pumped at a rate which did not allow full equilibration with the external CO₂, resulting in a diffusion-dependent response. Although this approach had excellent CO₂ sensitivity, slow or stopped-flow, which achieved equilibrium with the external solution, was less sensitive to diffusion and temperature and resulted in dramatically improved measurement precision⁸. The sensor design in Figure 2 required about 5 min. to achieve equilibrium between the indicator and external solution⁹. During each measurement cycle a solenoid pump was activated pushing new indicator solution into the membrane and flushing the CO₂-equilibrated solution into the fiber optic flow cell⁹. The SAMI solenoid pump delivers ~50 μL of solution per pulse, which was sufficient to flush out the cell and membrane.

Finally, to achieve the calibration-free system of the subject invention, the response must be calculated from a ratio of the absorbance of the analyte-selective reagent at two different wavelengths, the absorbances determined relative to a blank solution.

The sensor response in the subject calibration-free system is calculated from the analyte-sensitive reagent, or indicator absorbances at two different wavelengths. The wavelengths chosen correspond to the molar absorptivity maxima of the two indicator forms,

$$(1) \quad A_{\lambda} = -\log \frac{I_{\lambda}}{I_{\lambda 0}}$$

where A_λ is the indicator solution absorbance at wavelength λ , I_λ is the intensity transmitted through the reagent and $I_{\lambda 0}$ is the transmitted intensity through a blank solution. The chosen wavelengths correspond to the molar absorptivity maxima of measurements.

In an exemplified embodiment comprising a SAMI-CO₂ sensor, the sulfonephthalein, bromothymol blue (BTB) is the analyte-selective reagent or indicator solution. The two wavelengths of BTB are 434 nm for the acid, or protonated HL⁻ form, and 620 nm for the base, or unprotonated L²⁻ form (Figure 3). The sensor response could be based on the individual absorbances at either 434 or 620 nm but by combining the absorbances in a ratio, i.e. A_{620}/A_{434} . The sensor response A_R is therefore calculated by combining the absorbances at two different wavelengths of the indicator solution in a ratio, i.e. $A_R = A_{\lambda 1}/A_{\lambda 2}$. The response as shown herein is independent of cell pathlength and total indicator concentration, two potential sources of variability and drift.

The sensor response is calculated using an equation that relates the absorbance ratio directly to the indicator solution pH. In an exemplified embodiment using a SAMI-CO₂ sensor with BTB indicator, the absorbance ratio is A_{620}/A_{434} . The solution pH at infinite dilution (activity coefficients=1) can be described using a combination of the indicator equilibrium expression with Beer's law^{10,11},

$$(2) \quad \text{pH} = \text{pK}_a + \frac{\log [L^{2-}]}{[HL^{-}]}$$

with

$$(3) \quad \frac{[L^{2-}]}{[HL^{-}]} = \frac{A_R - \epsilon_{620a} / \epsilon_{434a}}{\epsilon_{620b} / \epsilon_{434a} - A_R \epsilon_{434b} / \epsilon_{434a}}$$

where $A_R = A_{620}/A_{434}$ and the subscripted ϵ 's represented the molar absorptivities for BTB with "a" the acid form of the indicator, and "b" the base form of the indicator. As shown in Figure 3, the absorbance spectra for the acid and base forms overlap and both indicator forms

contribute to the absorbances at the analytical wavelengths. These overlapping absorbances are accounted for in the derivation of Equation 3.

The SAMI response, R_{CO_2} , is calculated from Equations 2 and 3:

$$(4) \quad R_{CO_2} = -\log \left(\frac{A_R - \epsilon_{620a} / \epsilon_{434a}}{\epsilon_{620b} / \epsilon_{434b} - A_R \epsilon_{434a} / \epsilon_{434a}} \right) = + pK_a - pH.$$

From this equation, it is apparent that the sensor response is a fundamental property of the analyte-selective reagent chemistry. The response therefore has a physical meaning, representing the indicator solution pH offset from the pK_a . Equation 4 also shows that the response R_{CO_2} is only dependent upon the molar absorptivities and absorbance ratio. In turn, the absorbance ratio A_R is dependent upon the original solution alkalinity, ambient pCO_2 and temperature. Thus, every SAMI and likewise every reagent-based optical chemical sensor/analyzer whose reaction results in two light absorbing forms run under the calibration-free conditions of the subject invention will have an identical response for an identical indicator solution assuming good wavelength and absorbance accuracy.

The calibration-free system of the subject invention requires careful solution preparation, wavelength calibration and stray light rejection. The following provides specific examples of means by which these parameters were controlled for the calibration-free system described in the exemplified embodiment. Similar choices in detector size, photodiode type, solution preparation, handling and storage would be apparent to those skilled in the art in designing other calibration-free systems.

Good absorbance, i.e. photometric accuracy, is achieved by careful design and evaluation of the optical system. Detector size should be selected to increase the signal-to-noise (S/N) ratio without significantly compromising linearity due to inadequate resolution. For example, the SAMI uses a miniature f/2.5 spectrograph with 10 nm mm^{-1} reciprocal linear dispersion (Model MS10, American Holographic, Littleton, MA) and three photodiode detectors (G1962 and S2386-5K, Hamamatsu Corp., Bridgewater, NJ). Detectors are

positioned with the center wavelength at 434, 620, and 740 nm in the spectrograph focal plane. Detector photosensitive surface areas are 2.3, 2.4 and 2.4 mm² at 434, 620, and 740 nm, respectively, resulting in a resolution of ~23-24 nm. The S/N at 434, 620 and 740 is typically ~2500, 4500, and 4500, respectively.

5 In an exemplified embodiment, a SAMI-CO₂ sensor comprises three detectors, two standard silicon detectors and one GaP photodiode in a diffraction grating based system. Other detector arrangements including interference filter based light separation systems and scanning wavelength instruments also are suitable for use in the subject calibration-free system. Likewise, detectors can be arranged in a photodiode array within the reagent-based
10 optical chemical sensors/analyzers. It is only necessary that these systems provide photometric accuracy.

Photometric accuracy in spectrophotometric measurements can be limited by stray light. Tungsten light sources emit considerably more light in the near-infrared (NIR) than in the visible spectrum and measurements at short wavelengths, such as 434 nm, are especially
15 susceptible to stray NIR light. Stray light levels, evaluated with a 600 nm long pass filter, were found to be as high as 20% at 434 nm in an exemplified embodiment. A heat-absorbing filter (005GF13-25, Andover Corp., Salem, NH) placed at the spectrograph filter optic input reduced stray light to 0.1%. This filter however significantly reduced the S/N at 740 nm. In a specific embodiment, a GaP photodiode (G1962, Hamamatsu) that is insensitive to NIR
20 light was used in place of the broad-response Si photodiode at 434 nm. The GaP photodiode reduced stray light to less than 0.04% at 434 nm while maintaining a S/N of over 2500. As an additional check on absorbance accuracy each spectrograph was routinely evaluated with neutral density filters. Absorbances typically agree with the filters to within +/- 0.003 a.u. based on these evaluations, which was within the reproducibility of the neutral density filter
25 measurements.

Spectrograph absorbance accuracy also depends upon accurate wavelength calibrations. Thus, it is preferred that each 620 nm detector output is optimized in the lab with a 620 +/- 2nm bandpass filter. The other detectors should be positioned to correspond to 434 and 740 nm relative to the 620 nm detector, based on the grating dispersion. The

broad absorbance bands (Figure 3) and detector bandpass relax the need for wavelength accuracy better than 2-3 nm.

The analyte-selective reagent, sensing solution, or indicator solution of the sensors of the subject invention should be reproducibly prepared. In the exemplified embodiment, a solution of 50 μM BTB with 42 $\mu\text{eq l}^{-1}$ of NaOH was used as the sensing solution. The base was added to optimize the indicator pH response range⁹. The BTB and standardized NaOH were added to 1.00 kg deionized, degassed H_2O and the indicator solution was placed in polyethylene-coated aluminum bags. The indicator solution composition was checked by equilibrating it with a known $p\text{CO}_2$ and measurement of R_{CO_2} on a UV/VIS spectrophotometer.

The exemplified embodiment describes a SAMI- CO_2 response which is both reproducible between instruments and very stable the two conditions necessary for calibration-free performance. Although this embodiment departs from the conventional single-ended optrode design, similar performance can be expected for optrodes if the optrode is configured as in conventional colorimetric measurements, i.e. where the reagent is renewed and true solution absorbances are determined. Non-renewable ROCS have no means for determining I_0 and can therefore not take advantage of the improved performance offered by this approach. However, most fixed reagent sensor designs can be readily modified to accomodate the pump, valve and additional tubing. A wide variety of pumping mechanisms and valves are now available^{15, 16} and they have proven to be very reliable for long-term measurements in harsh environments. Many of the ROCS described have a membrane which traps the indicator solution. The ROCS need not contain such a membrane but sensors and analyzers in which the reagent is mixed directly with the analyte are also suitable for use in the subject calibration-free system.

The ratio techniques employed by the system of the subject invention, eliminates dependence on the system's operational parameters such as pathlength, light intensity, and the detector response function. Multi-wavelength detection and use of absorbance ratios take advantage of the two forms of a colorimetric reagent. Many colorimetric ROCS sensors

utilize reagents of this type including those, for example, for pH, gases, metal ions, anions, organics, and biochemical compounds^{17, 18, 19, 20}.

Calibration-free operation is also facilitated if the sensor response is based on an equilibrium between the reagent solution and external sample. The sensor response becomes diffusion-independent in this case and is insensitive to changes in the diffusional boundary layer around the sensor membrane. This simplification also makes it possible to model the response based solely upon thermodynamic considerations. If the thermodynamic constants are available, such models are useful for evaluating the sensor response and detecting systematic measurement errors²¹.

The calibration-free system of the subject invention can also be used with ROCs based on fluorescent reagents. The fundamental response of these ROCS depends on the fluorophore quantum efficiency and concentration. As in any intensity-based measurement, the signal output reflects the detector response, light source output and additional instrumental parameters²². A fluorescence ratio of two forms of the fluorophore can be used²³. Since the two forms are detected at different wavelengths however the ratio would not correct for wavelength dependent throughput and detector response. This would present an obstacle to designing sensors with an identical response. If the fluorophore did not exist in two forms, as found in quenching based O₂^{24, 25, 26}, the ratio approach could only be used if an additional O₂ insensitive fluorophore was included in the sensing solution.

Other absorbance-based sensors, such as optrodes, can be designed and operated in a similar fashion, making calibration-free optical chemical sensors available for a wide range of biomedical, industrial and environmental applications. Additionally, calibration-free ROCs can also be developed based on other approaches. Fluorescence lifetime-based ROCS are one example of a promising alternative²⁷. Furthermore, the performance of non-renewable ROCS continues to be improved through innovative fabrication techniques^{24, 26}.

The subject calibration-free sensors still require initial characterization of the response. After the response is thoroughly evaluated and well-established, a single set of regression coefficients can be used to calculate analyte concentration from any one of the identically-designed sensors. Calibration-free sensors undoubtedly will require occasional checks on the

instrument response. A single calibration standard could be used to determine if the instrument response matches the expected response and, if they do not agree, further evaluation of the instrument optical system or indicator chemistry may be necessary.

5 The following examples are offered to further illustrate but not limit both the compositions and the method of the present invention. All percentages are by weight and all solvent mixture proportions are by volume unless otherwise noted.

Example 1-Determination of the sensor to sensor reproducibility.

10 The following results demonstrate that all sensors operated, as described above, have an identical response. The SAMI response (R_{CO_2}) was determined in a water-filled thermostated chamber. Variable gas concentrations were obtained by mixing a 1600 ppm CO_2 standard with CO_2 -free air using two mass flow controllers⁹. The chamber headspace was continuously monitored by a nondispersive infrared CO_2 analyzer (NDIR) (Model LI-6251, LiCOR, Inc., Lincoln, NE) calibrated with N.I.S.T. traceable CO_2 gas standards (Air Liquide, Long Beach, CA). A circulating water pump mixed the equilibrator contents to insure complete equilibration. Equilibration temperature and barometric pressure were also monitored and used in the NDIR analyzer mole fraction (X_{CO_2}) calculations^{1,9}. The NDIR pCO_2 was calculated using,

20 (5)
$$pCO_2 = X_{CO_2(Wet)} P$$

where $X_{CO_2(Wet)}$ was the CO_2 mole fraction in water-saturated air determined by the NDIR and P was the barometric pressure.

25 Three identically-designed SAMIs were compared. Prior to determining the response curves, each SAMI was carefully tested for wavelength and photometric accuracy and the same indicator solution was loaded into the reagent bags for each instrument. The 3 SAMI responses were then sequentially determined as described in Example 1. These results, presented in Figure 4, show a nearly identical response between the different instruments.

The R_{CO_2} from the 3 SAMIs at 20.5°C range from 0.45 to 0.85, or a pH of ~0.40 (Equation 4), from 200-650 $\mu\text{atm } pCO_2$. Coefficients from curve fitting are shown in Table 1 and the pCO_2 s calculated for different R_{CO_2} s using these equations are shown in Table 2.

Table 1. Curve fitting parameters for SAMI response date in Figures 4 and 8.

Coefficients	SAMI 5 10/29/97	SAMI 6 10/21/97	SAMI 7 10/23/97	Theoretical Curve	SAMI 5 01/11/98
a	0.1076	0.1913	0.1437	0.1369	0.1087
b	0.2391	-0.2444	0.0317	0.0655	0.2539
c	-0.6606	0.0264	-0.3682	-0.4798	-0.7015

Coefficients from a curve fit of the form: $R_{CO_2} = a(\log pCO_2)^2 + b(\log pCO_2) + c$

Table 2. Calculated pCO_2 s (μatm) for different R_{CO_2} s using the equations in Table 1.

R_{CO_2}	SAMI 5 10/29/97	SAMI 6 10/21/97	SAMI 7 10/23/97	SAMI 5 01/11/98	Std. Dev. *
0.40	166	150	160	167	8.1
0.45	194	181	190	195	6.7
0.50	227	217	224	227	5.1
0.55	264	258	263	263	3.2
0.60	307	305	307	305	1.2
0.65	356	358	358	352	1.2
0.70	412	418	415	405	3.0
0.75	475	485	480	466	5.0
0.80	546	561	553	534	7.5
0.85	627	645	636	612	9.0

*This is the standard deviation of the calculated pCO_2 for SAMI 5, SAMI 6, and SAMI 7.

The estimated $p\text{CO}_2$ s from the three response curves agreed to within the uncertainty of the calibration procedure (1.8 μatm ave. standard deviation for the data in Table 2) in the range from 300-400 μatm which is the most common range encountered in marine studies.

The absorbance data used to generate Figure 4 illustrate the importance of using absorbance ratios (Figure 5). The absorbances differ between SAMIs by as much as 0.05 a.u. The consistently high and low absorbances between SAMIs suggested that the differences originate from optical pathlength differences, with SAMI 5 having the longest and SAMI 6 the shortest pathlength. The pathlength of the fiber optic cell (Figure 2) is 0.75 cm but the pathlength can vary between SAMIs due to imprecise positioning of the fibers in the sealed fittings. Clearly, sensors that are based on absolute absorbances must have very carefully controlled pathlengths to achieve reproducible sensor-to-sensor performance. As indicated by the convergence of the response curves in Figures 4 and 5, the SAMI response (R_{CO_2}) is insensitive to pathlength variability.

Most chemical sensors have a temperature dependent response and it is important to accurately quantify this dependence and correct for it in the recorded signal. The SAMI temperature response was evaluated by determining both the experimental and theoretical R_{CO_2} at different temperatures and $p\text{CO}_2$ s (Figure 6). The sensor temperature dependence originates primarily from the temperature-dependent CO_2 solubility (a solution equilibrated with the same $p\text{CO}_2$ will have a different pH at different temperatures). R_{CO_2} decreases as temperature increases as a result of this effect. The experimental temperature response followed the expected trend (Figure 6) although the offset was present between the experimental and theoretical R_{CO_2} as discussed above. The implications of Figure 6 are that the temperature coefficient is significant and that the magnitude depends upon the $p\text{CO}_2$. During previous field deployments the SAMIs were calibrated as closely as possible to the expected seawater temperature to minimize the temperature correction.

Example 2-Evaluation of long-term stability.

A reproducible sensor-to-sensor response as shown in Figure 4 is one performance characteristic necessary for calibration-free operation. A second equally important quality is

that the response must not change, or drift, over time. Drift minimized in the SAMIs using three techniques: renewing the indicator reagent, periodic measurement of solution blanks, and use of absorbance ratios. Blanks are necessary not only to calculate absorbances but to also correct for wavelength-dependent intensity changes.

5 Drift improvements by renewing the reagent, measuring blanks, and using absorbances ratios has not been systematically compared to the performance of ROCS that do not employ these techniques. However, an indirect comparison is provided from the literature where sparse long-term stability data have been reported for non-renewable intensity-based ROCS (see for example the recent SPIE volume *Chemical, Biochemical and Environmental Fiber*
10 *Sensors IX*, June 1997). This summary is based on the criteria that a rigorous evaluation of long-term stability consists of regular accuracy checks without recalibration for a period greater than 1 week. A more specific example is given by examination of ROCS CO₂ sensors developed for oceanographic applications^{12, 13, 14}. Almost no long term data have been presented for these sensors, which are all based on fixed reagents. In contrast, the SAMIs
15 have demonstrated excellent stability from the very early stages of development^{8,9}. A month-long *in situ* seawater test found no detectable drift in the response⁹ and recent laboratory studies have shown no significant change in the response with time (Figure 7). Although the two curves in Figure 8 are not identical, the difference in *p*CO₂ determined from the curve fit equations is very small over the typical oceanographic range (Table 2). Verification of
20 accuracy during ocean mooring deployments had been more difficult due to infrequent visits by supporting research vessels and spatial variability between the ship and the mooring. However, two SAMIs that were deployed on an ocean mooring off Cape Hatteras during 1996 give an indication of the long-term stability in the field (Figure 8). The two *p*CO₂ signals, which were calculated from the same R_{CO2}- *p*CO₂ response curves, show no
25 systematic deviation with time over the ~50 days when the two instruments were operational. The large periodic differences between the two instruments correspond to temperature differences between the instrument depths indicating the presence of density stratification and associated concentration gradients with depth (DeGrandpre, unpubl., 1998). The combined data sets in this case provide an evaluation of the long-term stability in the field.

It should be understood that the examples and embodiments described herein are for illustrative purposes only and that various modifications or changes in light thereof will be suggested to persons skilled in the art and are to be included within the spirit and purview of this application and the scope of the appended claims.

For reference

References

- 1 MacCraith, B.D.; McDonagh, C.; McEvoy, A.K.; Butler, T.; O'Keefe, G.; Murphy, V.J. *Sol-Gel Sci. Tech.* 1998, 8, 1053-1061.
- 2 Spichiger-Keller, U.E. *Chemical Sensors and Biosensors for Medical and Biological Applications*, Wiley-VCH: Weinheim, 1998.
- 3 Angel, S.M. *Spectroscopy* 1987, 2 38-50.
- 4 Berman, R.J.; Christian, G.D.; Burgess, L.W. *Anal. Chem.* 1990, 62, 2066-2071.
- 5 Inman, S.M.; Stromvall, E.J.; Lieberman, S.H. *Anal. Chem Acta* 1989, 217, 249-262.
- 6 Vurek, G.G.; Fuestel, P.J.; Severinghans, J.W. *Ann. Biomed. Eng.* 1983, 11, 499-510.
- 7 DeGrandpre, M.D. *Proc SPIE-Int. Soc. Opt. Eng.* 1991, 1587, 60-66.
- 8 DeGrandpre, M.D. *Anal. Chem.* 1993, 65, 331-337.
- 9 DeGranpre, M.D.; Hammar, T.R.; Smith, S.P.; Sayles, F.L. *Limnol. and Oceanog.* 1995, 40, 969-975.
- 10 Byrne, R.H.; Breland, J.A. *Deep-Sea Res.* 1989, 36, 803-810.
- 11 Clayton, T.D.; Byrne, R.H. *Deep-Sea Res.* 1993, 40, 2115-2129.
- 12 Goyet, C.; Walt, D.R.; Brewer, P.G. *Deep-Sea Res.* 1992, 39, 1015-1026.
- 13 Goswami, K.; Kennedy, J.A.; Dandge, D.K.; Klainer, S.M.; Tokar, J.M. *Proc. SPIE-Int. Soc. Opt. Eng.* 1990, 1172, 225-232.
- 14 Lefevre, N.; Ciabrini, J.P.; Michard, G.; Brient, B.; DuChaffaut, M.; Merlivat, L. *Mar. Chem.* 1993, 42, 189-198.
- 15 Jannasch, H.; Johnson, K.S.; Sakamoto, C.M. *Anal. Chem.* 1994, 66, 3352-3361.
- 16 Weeks, D.A.; Johnson, K.S. *Anal. Chem.* 1996, 68, 2717-2719.
- 17 Peterson, J.L.; Goldstein, S.R.; Fitzgerald, R.V.; Buckhold, D.K. *Anal. Chem.* 1980, 52, 864-869.
- 18 Zhou, Q.; Kritz, D.; Bonnell, L.; Sigel, G. *App. Opt.* 1989, 28, 2022-2025.
- 19 Chau, L.K.; Porter, M.D. *Anal. Chem.* 1990, 62, 1964-1971.
- 20 Radloff, D.; Matern, C.; Plaschke, M.; Simon, D.; Reichert, J.; Ache, H.J. *Sens. Actuators B* 1996, 35-36, 207-211.
- 21 DeGrandpre, M.D., *Anal. Chem.* 1999, 71, 1152-1159.

- 22 Ingle, J.D.; Crouch, S.R. *Spectrochemical Analysis*. Prentice-Hall: New Jersey, 1988.
- 23 Thompson, R.B.; Jones, E.R. *Anal. Chem.* 1993, 65, 730-734.
- 24 McDonagh, C.; MacCraith, B.D.; McEvoy, A.K. *Anal. Chem.* 1998, 70, 45-50.
- 25 Wolfbeis, O.S.; Posch, H.E.; Kroneis, H.W. *Anal. Chem.* 1985, 57, 2556-2561.
- 5 26 Klimant, I.; Meyer, V.; Kuhl, M. *Limnol. Oceanogr.* 1995, 40, 1159-1165.
- 27 Draxler, S.; Lippitsch, M.E. *Proc. SPIE-Int. Soc. Opt. Eng.* 1993, 2085, 61-67.

Table 1. Demographic characteristics of the study population	
Age (years)	65.0 ± 1.5
Gender	
Male	50.0%
Female	50.0%
Education (years)	12.0 ± 1.0
Marital status	
Married	60.0%
Single	40.0%
Occupation	
Retired	70.0%
Unemployed	30.0%
Income (USD/month)	1,200.0 ± 200.0
Health status	
Good	60.0%
Fair	40.0%
Poor	0.0%
Comorbidities	
Hypertension	30.0%
Diabetes	20.0%
Cholesterol	10.0%
Smoking status	
Smoker	10.0%
Non-smoker	90.0%
Alcohol consumption	
Regular	5.0%
Occasional	15.0%
Never	80.0%